Journal of Materials Science: Materials in Electronics (2020) 31:12109–12115
https://doi.org/10.1007/s10854-020-03757-1

Metal halide-based photodetector using one-dimensional $MAPbI_3$ micro rods

Ehsan Raza[1] · Zubair Ahmad[1] · Arti Mishra[1] · Fakhra Aziz[2]

Received: 3 April 2020 / Revised: 5 June 2020 / Accepted: 7 June 2020 / Published online: 13 June 2020

Abstract

In the present work, we report the fabrication of a photodetector using methylammonium lead iodide perovskite ($MAPbI_3$) micro rod. Photosensitivity of the Ag/$MAPbI_3$/Ag photodetector has been studied under various light intensities ranging from 10 to 100 mW/cm^2. The $MAPbI_3$ perovskite micro rod-based photodetector shows a high on/off ratio (4.47×10^5), and fast response & recovery times (2.7 ms, each), as compared to the photodetectors using perovskite films. This work could initiate new perspectives for perovskite micro rods to be employed in high-performance optoelectronic devices.

1 Introduction

Photodetectors refer to optoelectronic devices that can convert incident light into electrical signals, are significant functional elements in a variety of areas such as environmental monitoring, fire deduction, and security, optical communications, space exploration, and video imaging [1, 2]. Different classes of semiconductor materials have been employed in photodetectors, such as GaN, InGaAs, Si, ZnO, carbon nanotubes, conjugated polymers, and quantum dots [3]. Devices based on these materials require complex and expensive manufacturing cost and mechanical inflexibility.

During the last decade, metal halide perovskite materials acquired a great interest of researchers due to their broad applications in photovoltaic and optoelectronic devices [4]. This class of material has been emerged as a potential candidate towards the future of plenty of photovoltaic and optoelectronic devices due to its outstanding high performance, low cost, and solution processability [5]. Among numerous available metal halides, methylammonium lead iodide ($MAPbI_3$) has been widely investigated for photovoltaic and photo-sensing applications [6].

Indeed, perovskite materials have achieved remarkable efficiency in photovoltaic devices, but these solar cells suffering long-term stability issues. Since the photodetector applications don't require high power conversion efficiency and focus is instead given on the sensitivity of the device, cost-effectiveness, and ease of fabrication as compared to their counterparts, including Si or InGaAs based predominant photodetectors [7, 8]. Further, perovskite materials offer extraordinary features such as high charge carrier mobilities [9], light absorption over a broad spectral range [10], high absorption coefficient, flexibility, and low cost [11]. These characteristics consider perovskite material as a favorable contender for highly efficient photodetectors.

Many reports were published by numerous research groups based on the employment of perovskites as fast and highly sensitive photodetectors, revealing a broad spectral behavior from ultraviolet (UV) to visible (vis) wavelength range [12–14]. For example, Dong et al. [15] fabricated solution-processed broadband $MAPbI_3$ perovskite-based photodetectors and demonstrated fast response speed and high responsivity. Zhao and co-workers made organometal halide perovskite thin films on top of interdigitated (IDT) patterned gold (Au) electrodes and demonstrated highly sensitive and fast response speed photodetectors [16].

$MAPbI_3$ can attain either thin-film or crystal form; however, the perovskite crystals demonstrate far better behavior than the crystalline thin films [17, 18]. Moreover, nano- and micro-structured $MAPbI_3$ are more beneficial for optoelectronic applications due to their tunable optical bandgap, absorption coefficient, and carrier diffusion length [19]. The optical and electronic properties of perovskite crystals can be further tuned depending upon crystal structures (confined structure of lower dimensions

✉ Zubair Ahmad
zubairtarar@qu.edu.qa

1 Center for Advanced Materials (CAM), Qatar University, P.O.Box 2713, Doha, Qatar

2 Department of Electronics, Jinnah College for Women, University of Peshawar, 25120 Peshawar, Pakistan

give more tunability) [20]. Perovskite halides can form three-dimensional (3-D), two-dimensional (2-D), one-dimensional (1-D), or zero-dimensional (0-D) networks with the same unit structure [21]. Therefore, they can be employed innovatively to overcome conventional semiconductors pitfalls [22, 23]. Particularly, $MAPbI_3$ 1-D crystals offer a variety of attractive features such as length in the range of 3–4 mm, fewer heterostructure defects, and growth from simple solution-based technique [24]. Indeed, well defined $MAPbI_3$ crystal structures provide precise information about phase purity, connectivity between atoms, the surface to volume ratio, light absorption, etc. Randomly distributed perovskite crystalline structures result in deteriorated device performance [25]. Hence, consistent regular distribution and alignment of the crystalline structures make them more appropriate for the wavelength-specific photodetectors application [26].

The extensive use of perovskite wires in photodetectors, employing different fabrication techniques, has been reported in recent years. Horváth et al. [27] have fabricated $MAPbI_3$ nanowires-based photodetectors by a low-temperature solution processing slip-coating technique. In their work, they have made a comparison between the devices fabricated from nanowires and spin-coated films and have demonstrated distinct features of nanowires-based devices. Moreover, Deng et al. [18] have prepared high-performance photodetectors using perovskite small-diameter nanowires synthesized by a template method for control growth distributions of the monolayer. In the present work, the $MAPbI_3$ 1-D micro rods have been successfully employed to fabricate the photodetector. The facile solution processing technique is used to grow 1-D micro rods of $MAPbI_3$ perovskite, and their morphological and structural properties have been investigated as well.

2 Materials and methods

Lead (II) iodide (PbI_2) and methylammonium iodide (MAI) were purchased from Sigma-Aldrich and TCI Chemicals (Japan), while the Dimethylformamide DMF (anhydrous, 99.8%) and isopropanol (IPA) were obtained by Agros chemicals and VWR Prolab chemicals, respectively. All the chemicals were used as received. 1 M solutions of each PbI_2 and MAI were prepared in DMF and IPA, separately. The solutions were mixed in the 2:1 volumetric ratio to make the $MAPbI_3$ solution. Initially, the thick precipitates of perovskite were formed; however, simultaneous stirring and heating at 400 rpm and 70 °C produced a clear yellow $MAPbI_3$ solution. The resultant $MAPbI_3$ solution was allowed to cool down to the room temperature, at a prolonged rate (~ 10 °C/h), to form $MAPbI_3$ micro rods. The length of micro rods seems to increase within the solution in the vibration-free environment. Figure 1a demonstrates the stepwise synthesis of one-dimensional $MAPbI_3$ micro rods.

Commercially available pre-patterned interdigitated ITO/glass substrates (S161) were purchased from Ossila. The thickness of ITO on the glass substrate was 100 nm. Each substrate with dimensions (20 mm x 15 mm) (see the ITO/glass substrate image in the supplementary data file) consists of the five ITO based interdigitated sensation electrodes, while the each interdigitated sensation electrode consists of three channels with a dimension of 30 mm x 50 µm. An individual $MAPbI_3$ rod was placed over the pre-patterned ITO coated substrates. The two ends of the rod were fixed using silver (Ag) paste to produce $Ag/MAPbI_3/Ag$ photodetector. Figure 1b shows the device structure of one-dimensional $MAPbI_3$ microrod based $Ag/MAPbI_3/Ag$ photodetector. The surface morphology of the micro rods was performed using a field emission scanning electron microscope (FESEM). *I-V* characterization of the prepared device was recorded under different light intensities (10–100 mW/cm^2) using an Oriel

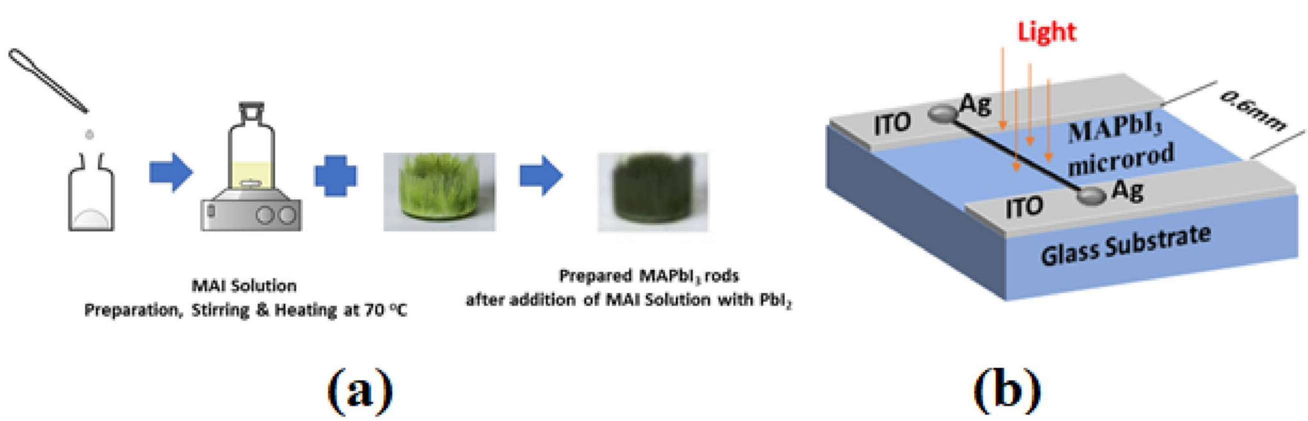

Fig. 1 **a** A stepwise synthesis procedure for the preparation of MAPbI3 micro rods. **b** Device structure of MAPbI3 microrod based photodetector

AAA solar simulator (Newport) and a Keithley 2400 source measuring unit (SMU).

3 Results and discussion

Figure 2 shows field emission scanning electron microscope (FESEM) images of MAPbI3 micro rods at different magnifications. The FESEM micrographs exhibit the porous structure of MAPbI3 microcrystalline rods with an approximate diameter of ~60 m while the length of the rod was 4-5 mm as described in our previous publication [24]. At higher magnification, the FESEM images reveal a well-aligned parallel arrangement of the perovskite submicron level crystals in the longitudinal direction. During the growth route, the crystals are joined in such a fashion that hollow regions are created. However, no adjacent cracks are visualized

The elemental composition of the micro rods was studied using EDS analysis. The results in Fig. 3 show the existence of Pb and I as major components. The two featured peaks at 2.32, and 10.5 keV corresponds to lead, while the peaks at 3.98 and 4.2 keV belong to iodine elements in $MAPbI_3$ crystals. In the case of $MAPbI_3$, the atomic composition of microcrystals demonstrates the presence of $MAPbI_3$ with I in the ratio of 1:2.1, which is consistent with $MAPbI_3$, confirming the formation of pure phases.

The photodetector (PD), shown in the schematic device structure of Fig. 1b, is fabricated using a one-dimensional perovskite microrod. The photoresponse measurements were performed in the dark and under light illumination at intensities between 10 and 100 $mWcm^{-2}$. The perovskite microrod absorbs incident photons with sufficient energy to generate excitons. Due to the applied and built-in electric field, the excitons are dissociated into electron-hole pairs (EHPs). The EHPs are, then, drifted to respective electrodes, which produce photo-generated current in the external circuit. Figure 4 shows current-voltage (*I*-*V*) characteristics of perovskite microrod based photodetector under multiple light intensities. The device responds well towards the incident light, even at low intensity of

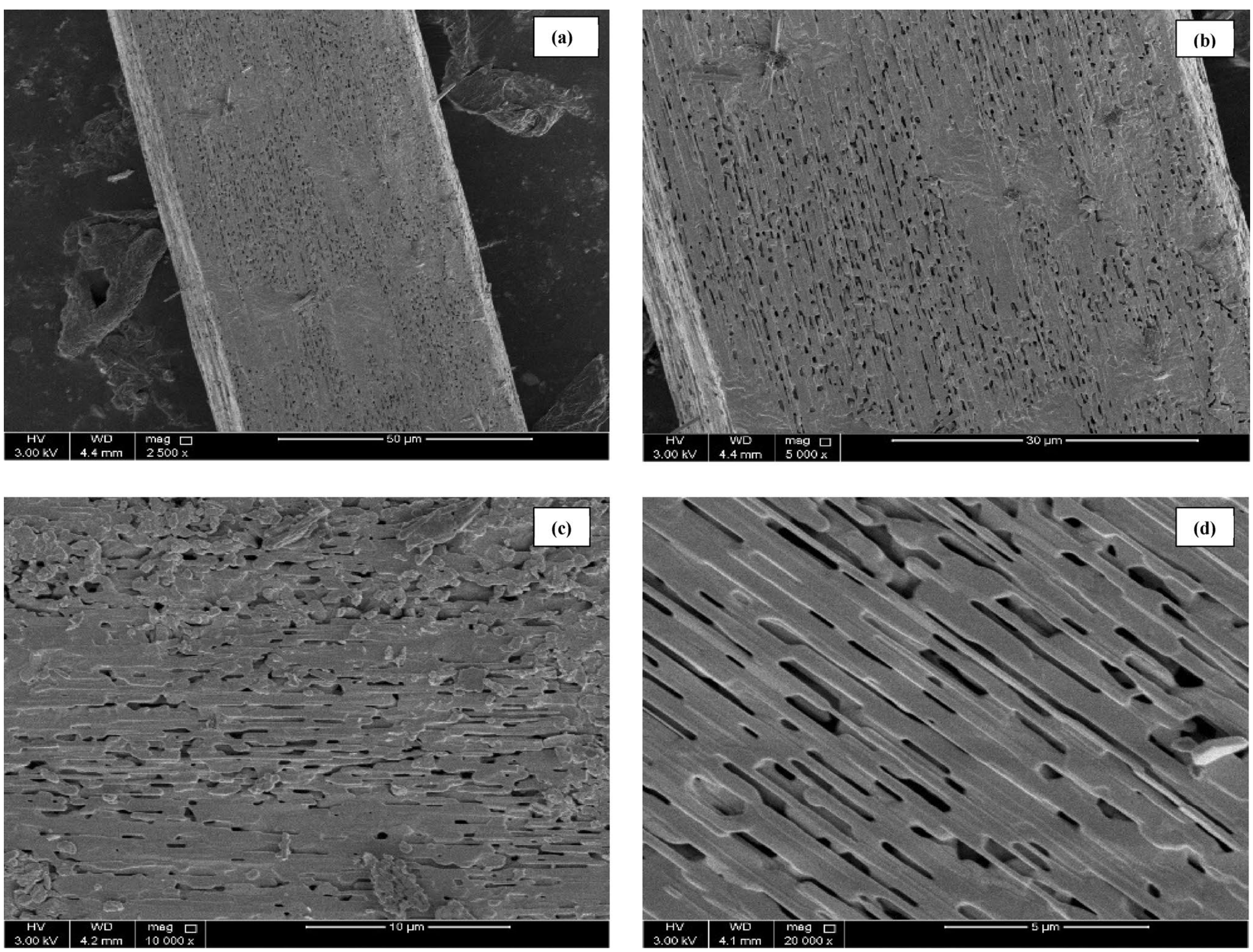

Fig. 2 FESEM images of the MAPbI3 micro rods at various magnifications

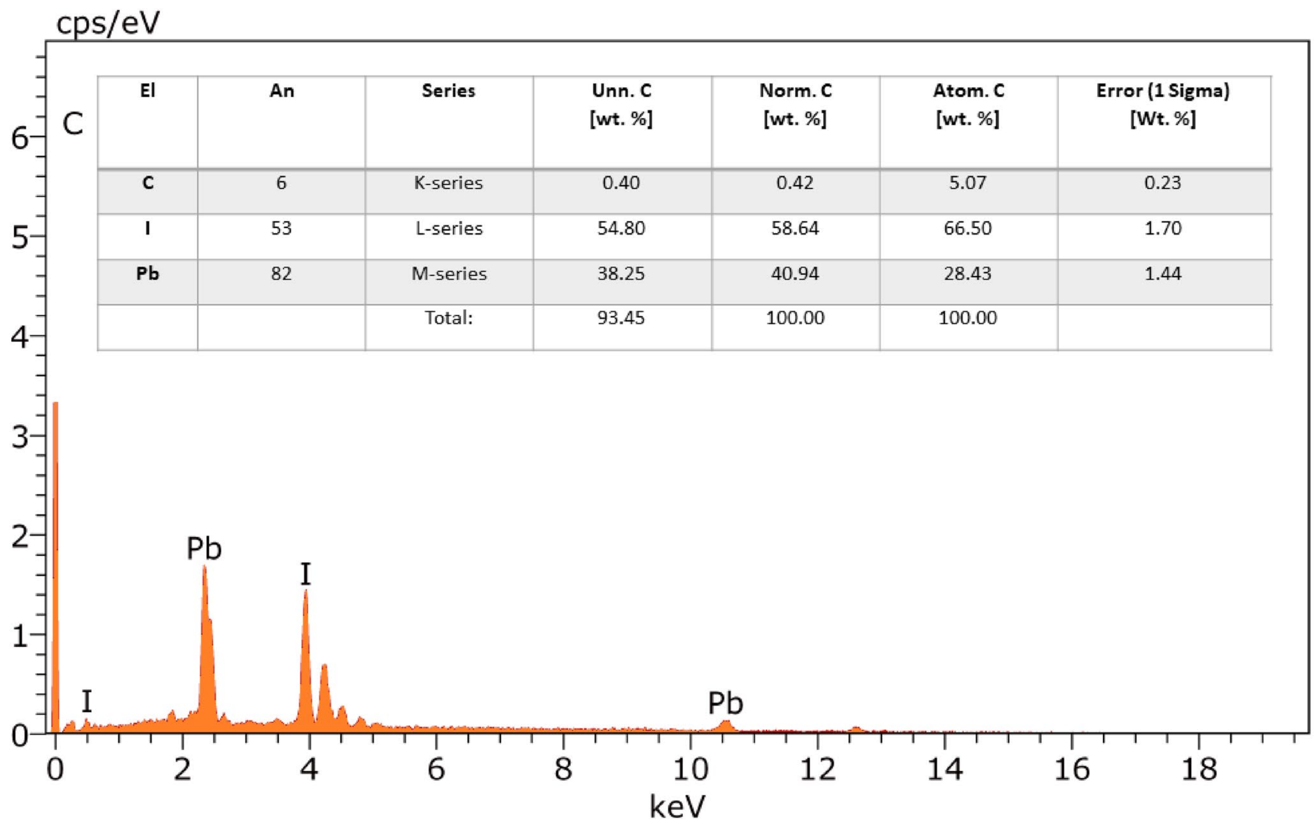

El	An	Series	Unn. C [wt. %]	Norm. C [wt. %]	Atom. C [wt. %]	Error (1 Sigma) [Wt. %]
C	6	K-series	0.40	0.42	5.07	0.23
I	53	L-series	54.80	58.64	66.50	1.70
Pb	82	M-series	38.25	40.94	28.43	1.44
		Total:	93.45	100.00	100.00	

Fig. 3 EDS spectra of MAPbI3 micro rods

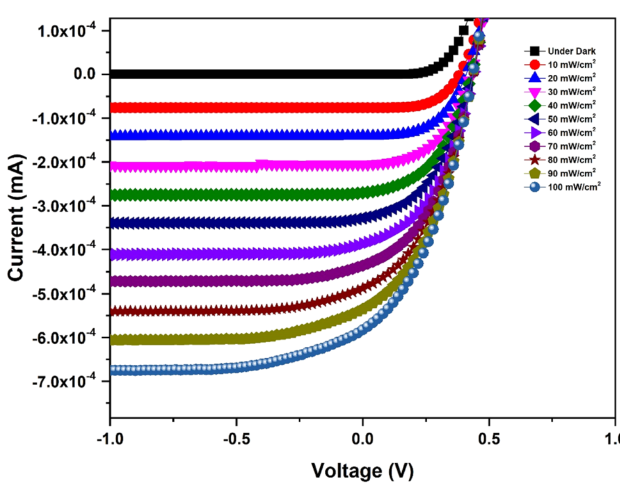

Fig. 4 Current vs. Voltage (I-V) characteristics of Ag/MAPbI3/Ag photodetector measured at various illumination intensities

incident light (~ 10 mW cm^{-2}), a noteworthy increase in the photocurrent is observed. The magnitude of photocurrent depends upon the generation of EHPs, which is directly correlated with the intensity of incident light, the greater the intensity, the greater the photocurrent. The photocurrent I_{light}, follows a power-law relationship with the intensity of incident light P according to the following equation [28].

$$I_{light} \alpha P^{\theta} \tag{1}$$

where P is the light intensity, and θ is photocurrent response. When light strikes on PD, the EHPs are generated and swept to the corresponding electrodes producing photocurrent even at zero bias. A considerable increase in the photocurrent of $MAPbI_3$ with increasing light intensities is observed in Fig. 4. The light to the dark current ratio (I_{light}/I_d) of the PD at 0.5 V operational bias has been calculated as $4.49 \pm 0.02 \times 10^5$. It is noteworthy that $MAPbI_3$ microrod based photodetector achieved an on-off ratio of about 10^5 that can be attributed to high carrier mobilities of holes and electrons [29]. The results, further, indicate that the EHPs are easily generated in $MAPbI_3$ microrod based PD under the influence of applied electric field between the electrodes.

Figure 5 reveals that the sensitivity of photocurrent is highly dependent on the operational bias voltage. A linear increase in the output current corresponding to the rise in

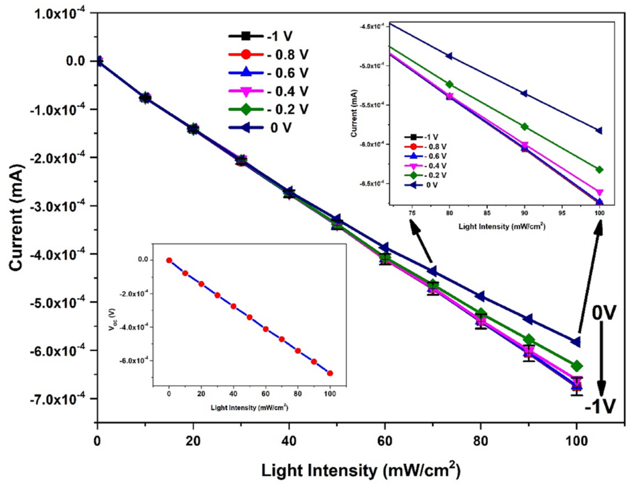

Fig. 5 Light Intensity vs. Current characteristics of Ag/MAPbI3/Ag photodetector measured at various biased voltages. The inset in the bottom left corner shows the open-circuit voltage of Ag/MAPbI3/Ag photodetector as a function of light intensity, while, the inset in the right top shows the magnified behavior at higher light intensity values. The average results of the three devices are presented in this Figure—the error bar indicates the standard deviation of the samples. The average value of the standard deviation was ±5%

the externally applied potential can be observed from the Figure. At lower illumination intensities, the lines of applied potential tend to overlap; however, at higher intensities, the current for the applied potential varies significantly [30]. Inset, given in Figure 5, shows the response of open-circuit voltage V_{oc} as a function of light intensities. The Figure demonstrates a linear increase in open-circuit voltage towards increasing light intensities. The voltage-dependent sensitivity S of the device can be calculated by the following equation [31]

$$S = \frac{I_{light} d}{PAV} \quad (2)$$

where I_{light} is the illuminated current value, d is the thickness of the rod, P represents the power of incident light, A defines the area of the rod, and V is the applied bias. Similarly, the responsivity R can be calculated using the equation given below [18, 30]:

$$R = J_p / P_{in} \quad (3)$$

Table 1 Comparison of $MAPbI_3$ microrod based photodetectors with the reported photodetectors using $MAPbI_3$ perovskite film and microwires

Material	Configuration	On/Off ratio	Response time (ms)	References
$MAPbI_3$	Film	--	200	[32]
$MAPbI_3$	microwires	4.02×10^3	--	[17]
$MAPbI_3$	microrod	4.47×10^5	2.7	Present work

In this case, J_p represents photocurrent density which can be further defined as $J_p = J_{light} - J_{dark}$ while the power of the incident light is represented by P_{in}. The sensitivity and responsivity were calculated as 8.67×10^{-5} Sm/W and 0.76 AW^{-1}, respectively. The responsivity of the $MAPbI_3$ microrod based PD is compared with that of the $MAPbI_3$ film and microwires in Table 1. It is observed that the microrod, used in this work, exhibits better responsivity as compared to microwires.

The light-dependent switching (on and off) response (at an external bias voltage of 0.4 V and 100 mW cm^{-2} illumination intensity) is presented in Fig. 6. The calculated response and recovery times were found as 2.7 ms, each. Our device exhibited superior performance in terms of on/off ratio and response time, as shown in Table 1. The on/off ratio of our device is 4.47×10^5, which is almost 100 times higher than the previous report on microwires [17]. Similarly, our device exhibited a response time of 2.7 ms, much faster than the thin-film based device, which is 200 ms [32].

4 Conclusion

In summary, one-dimensional $MAPbI_3$ micro rods were successfully fabricated to prepare the Ag/$MAPbI_3$/Ag photodetector, and their morphology was studied using FESEM. $MAPbI_3$ microrod based photodetector revealed outstanding performance in terms of sensitivity (8.67×10^{-5} Sm/W), on/off ratio ($4.47+0.02\times10^5$), and responsivity (0.76 AW^{-1}). Moreover, the photodetector exhibited a fast response and recovery time of ~2.7 ms each. The results show that the perovskite micro rods can be potentially implemented to fabricate sensitive and rapid photoelectric switches and photodetectors.

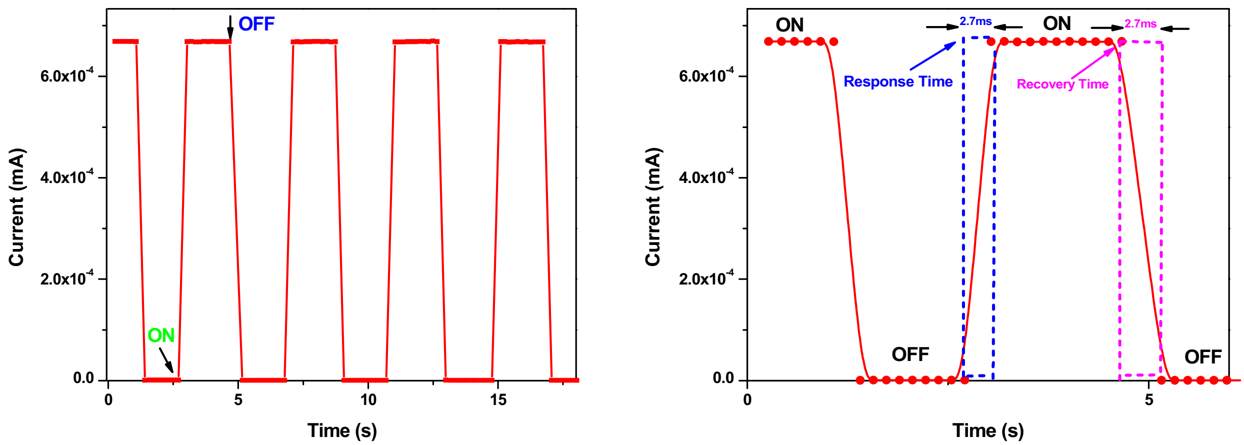

Fig. 6 Response and recovery times of Ag/MAPbI3/Ag photodetector

Acknowledgements Open Access funding provided by the Qatar National Library. The authors are highly thankful to the Center of Advanced Materials (CAM), Qatar University, for providing the lab facilities to perform this work.

Compliance with ethical standards

Conflict of interest The authors declare no conflict of interest.

References

1. C. Xie, F. Yan, Flexible photodetectors based on novel functional materials. Small **13**(43), 1701822 (2017)
2. M. Zhang, F. Zhang, Y. Wang, L. Zhu, Y. Hu, Z. Lou, Y. Hou, F. Teng, High-Performance Photodiode-Type Photodetectors Based on Polycrystalline Formamidinium Lead Iodide Perovskite Thin Films. Scientific reports **8**(1), 11157 (2018)
3. L. Dou, Y.M. Yang, J. You, Z. Hong, W.-H. Chang, G. Li, Y. Yang, Solution-processed hybrid perovskite photodetectors with high detectivity. Nature communications **5**, 5404 (2014)
4. S.-T. Ha, R. Su, J. Xing, Q. Zhang, Q. Xiong, Metal halide perovskite nanomaterials: synthesis and applications. Chemical science **8**(4), 2522–2536 (2017)
5. J. Sun, J. Wu, X. Tong, F. Lin, Y. Wang, Z.M. Wang, Organic/inorganic metal halide perovskite optoelectronic devices beyond solar cells. Advanced Science **5**(5), 1700780 (2018)
6. Y. Dong, Y. Zou, J. Song, X. Song, H. Zeng, Recent progress of metal halide perovskite photodetectors. Journal of Materials Chemistry C **5**(44), 11369–11394 (2017)
7. J. Kaniewski, J. Piotrowski, InGaAs for infrared photodetectors. Physics and technology. Opto-Electron. Rev. **12**(1), 139–148 (2004)
8. J. Michel, J. Liu, L.C. Kimerling, High-performance Ge-on-Si photodetectors. Nature photonics **4**(8), 527 (2010)
9. C. Wehrenfennig, G.E. Eperon, M.B. Johnston, H.J. Snaith, L.M. Herz, High charge carrier mobilities and lifetimes in organolead trihalide perovskites. Advanced materials **26**(10), 1584–1589 (2014)
10. W.S. Yang, J.H. Noh, N.J. Jeon, Y.C. Kim, S. Ryu, J. Seo, S.I. Seok, High-performance photovoltaic perovskite layers fabricated through intramolecular exchange. Science **348**(6240), 1234–1237 (2015)
11. H. Sun, T. Lei, W. Tian, F. Cao, J. Xiong, L. Li, Self-powered, flexible, and solution-processable perovskite photodetector based on low-cost carbon cloth. Small **13**(28), 1701042 (2017)
12. H.-R. Xia, J. Li, W.-T. Sun, L.-M. Peng, Organohalide lead perovskite based photodetectors with much enhanced performance. Chem. Commun. **50**(89), 13695–13697 (2014)
13. L. Dou, Y.M. Yang, J. You, Z. Hong, W.-H. Chang, G. Li, Y. Yang, Solution-processed hybrid perovskite photodetectors with high detectivity. Nature communications **5**(1), 1–6 (2014)
14. Y. Lee, J. Kwon, E. Hwang, C.H. Ra, W.J. Yoo, J.H. Ahn, J.H. Park, J.H. Cho, High-performance perovskite–graphene hybrid photodetector. Advanced materials **27**(1), 41–46 (2015)
15. R. Dong, Y. Fang, J. Chae, J. Dai, Z. Xiao, Q. Dong, Y. Yuan, A. Centrone, X.C. Zeng, J. Huang, High-gain and low-driving-voltage photodetectors based on organolead triiodide perovskites. Advanced materials **27**(11), 1912–1918 (2015)
16. F. Wang, J. Mei, Y. Wang, L. Zhang, H. Zhao, D. Zhao, Fast photoconductive responses in organometal halide perovskite photodetectors. ACS Appl. Mater. Interfaces **8**(4), 2840–2846 (2016)
17. C. Zhu, Y. Tang, F. Chen, A.G. Manohari, Y. Zhu, Z. Shi, C. Xu, Fabrication of self-assembly polycrystalline perovskite microwires and photodetectors. J. Cryst. Growth **454**, 121–127 (2016)
18. H. Deng, D. Dong, K. Qiao, L. Bu, B. Li, D. Yang, H.-E. Wang, Y. Cheng, Z. Zhao, J. Tang, Growth, patterning and alignment of organolead iodide perovskite nanowires for optoelectronic devices. Nanoscale **7**(9), 4163–4170 (2015)

19. R. Agarwal, C. Lieber, Semiconductor nanowires: optics and optoelectronics. Applied physics A **85**(3), 209 (2006)
20. S. Tongay, Preface to a Special Topic: 2D Materials and Applications. Applied Physics Reviews **5**(1), 010401 (2018)
21. T. Qiu, Y. Hu, F. Xu, Z. Yan, F. Bai, G. Jia, S. Zhang, Recent advances in one-dimensional halide perovskites for optoelectronic applications. Nanoscale **10**(45), 20963–20989 (2018)
22. V.G. Plekhanov, Lead halides: electronic properties and applications. Prog. Mater Sci. **49**(6), 787–886 (2004)
23. Q.A. Akkerman, G. Raino, M.V. Kovalenko, L. Manna, Genesis, challenges and opportunities for colloidal lead halide perovskite nanocrystals. Nat. Mater. **17**(5), 394–405 (2018)
24. A. Mishra, Z. Ahmad, F. Touati, R.A. Shakoor, M.K. Nazeeruddin, One-dimensional facile growth of MAPbI3 perovskite micro-rods. RSC Advances **9**(20), 11589–11594 (2019)
25. M.E. Roberts, N. Queraltó, S.C. Mannsfeld, B.N. Reinecke, W. Knoll, Z. Bao, Cross-linked polymer gate dielectric films for low-voltage organic transistors. Chem. Mater. **21**(11), 2292–2299 (2009)
26. W. Deng, X. Zhang, L. Huang, X. Xu, L. Wang, J. Wang, Q. Shang, S.T. Lee, J. Jie, Aligned single-crystalline perovskite microwire arrays for high-performance flexible image sensors with long-term stability. Adv. Mater. **28**(11), 2201–2208 (2016)
27. E. Horvath, M. Spina, Z. Szekrenyes, K. Kamaras, R. Gaal, D. Gachet, L. Forro, Nanowires of methylammonium lead iodide (CH3NH3PbI3) prepared by low temperature solution-mediated crystallization. Nano Lett. **14**(12), 6761–6766 (2014)
28. K., Rajpure, Effect of the buffer layer on the metal–semiconductor–metal UV photodetector based on Al-doped and undoped ZnO thin films with different device structures. Phys. Status Solidi A **212**(8), 1–9 (2015)
29. M. Grätzel, The light and shade of perovskite solar cells. Nat. Mater. **13**(9), 838 (2014)
30. E. Horváth, M. Spina, Z. Szekrényes, K. Kamarás, R. Gaal, D. Gachet, L.s. Forró, Nanowires of methylammonium lead iodide (CH3NH3PbI3) prepared by low temperature solution-mediated crystallization. Nano Lett. **14**(12), 6761–6766 (2014)
31. Q. Zafar, Z. Ahmad, Dual donor bulk-heterojunction to realize a quick and more sensitive organic visible photodector. J. Mater. Sci.: Mater. Electron. **29**(13), 11144–11150 (2018)
32. X. Hu, X. Zhang, L. Liang, J. Bao, S. Li, W. Yang, Y. Xie, High-performance flexible broadband photodetector based on organolead halide perovskite. Adv. Func. Mater. **24**(46), 7373–7380 (2014)